Electron tunneling based SEI formation model

ECS Transactions, 62 (1) 1-8 (2014)
10.1149/06201.0001ecst ©The Electrochemical Society

Electron tunneling based SEI formation model

Dongjiang Li[a,b], Dmitry Danilov[a], Zhongru Zhang[c], Huixin Chen[c], Yong Yang[b,c] and Peter H. L. Notten[a]

[a] Department of Chemical Engineering and Chemistry, Eindhoven University of Technology, 5600 MB Eindhoven, The Netherlands

[b] School of Energy Research, Xiamen University, Xiamen, 361005, China

[c] Department of Chemistry, Xiamen University, Xiamen, 361005, China

A new model, describing the capacity loss of C_6/$LiFePO_4$ batteries under open-circuit storage conditions has been developed. Degradation is attributed to the formation of a Solid Electrolyte Interface (SEI) at the surface of the graphite particles in the negative electrode. The model takes into account that the Solid Electrolyte Interface consists of an inner and outer SEI layer. The rate determining step of the SEI formation process is proposed to be electron tunneling through the inner SEI layer. The simulation results demonstrate that the capacity loss is dependent on the State-of-Charge (SoC), the electrode potential and storage time. The inner SEI layer was found to grow much slower than the outer SEI layer.

Introduction

Ageing of Li-ion batteries already draws the attention of many scientists and engineers for several decades. Though the basic principles of ageing processes in Li-ion batteries are well known, a complete mathematical description of this complex and multi-stage process is not yet available. It is commonly accepted that the formation of the Solid Electrolyte Interface (SEI) at the surface of graphite particles is one of the main reasons for the capacity loss in Li-ion batteries. The SEI plays, however, a dual-role in the battery performance. On the one hand, it protects the negative electrode from solvent co-intercalation, which could cause exfoliation of the graphite layers. On the other hand, it consumes cyclable lithium inside the cell, which leads to irreversible capacity losses. Though a lot of work have been done to study the SEI by experimental methods (1-19), a detailed theoretical understanding of the SEI formation process is still lacking due to its complexity. The formation process was found to be dependent on the composition of the electrolyte, the electrode potential and electrode surface morphology.

The structure of the SEI layer has been investigated by many researchers. Most recent experimental results show that the SEI layer consists of a compact inner layer and a more porous outer layer, which are mainly composed of inorganic Li salts and organic Li species, respectively (1-3, 15, 19, 20). The inner SEI layer is dense and is considered to isolate the graphite surface from direct contact with the electrolyte, favorably preventing

solvent co-intercalation into graphite. The inner SEI layer has good ionic conductivity but is considered to be electronically highly resistive.

While modeling is an efficient way to study the SEI formation, only a few studies are related to the SEI growth mechanism (20-26) and these studies are still subject of debate. Some researchers assumed that the electron diffusion process was rate determining (21) while others considered solvent diffusion to be rate limiting (25, 26). In the present work, a new SEI formation model is proposed, which is based on electron tunneling through the inner SEI layer. The model predicts the capacity losses observed during storage.

SEI formation mechanism

The SEI formed after battery activation includes two distinctive parts, the inner layer and outer layer. The inner SEI layer is composed of inorganic salts which form a dense structure on the graphite surface, while the outer SEI layer is composed of organic Li salts which have a highly porous structure (2). It is generally assumed that the solvent molecules (S) can easily pass the highly porous outer layer while these cannot penetrate the inner layer (25, 27). The inner SEI layer is a good insulator, but electrons can still tunnel through this layer when the thickness is sufficiently small. The solvent is immediately reduced when electrons arrive at the inner layer surface. Consequently, the reaction products increase the thickness of both the inner and outer layer. The SEI formation reaction under open-circuit, storage, conditions is schematically shown in Fig. 1.

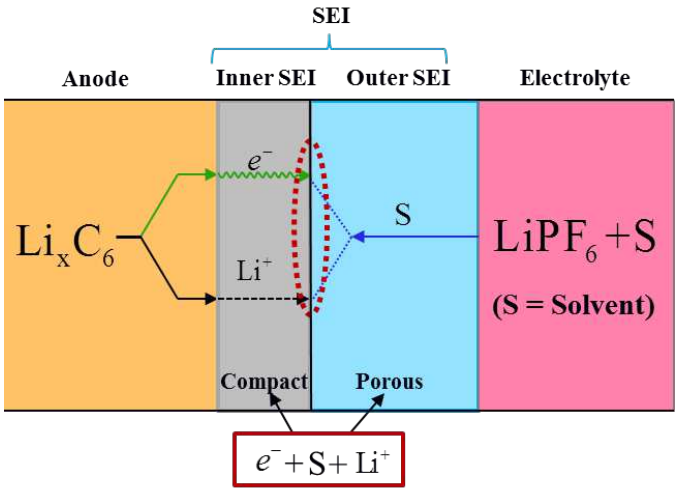

Fig. 1. Schematic representation of the SEI formation mechanism during storage.

Since under storage conditions no external current is flowing, reduction of the solvent must be an electroless process, implying that the electrons should be delivered by oxidation lithium stored inside the graphite electrode. The corresponding oxidation and reduction reactions involved in the SEI formation can be expressed by

$$Li_xC_6 \rightarrow Li_{x-y}C_6 + ye^- + yLi^+ \quad , \qquad [1]$$

and

$$S + ye^- + yLi^+ \rightarrow yLiR + gas \quad , \qquad [2]$$

respectively, where R represents the organic species (partly) composed of the organic solvents and gas is represented in general terms as the composition of the gas is strongly dependent on the conditions, *e.g.* ethylene in case of EC solvent. The complete electroless reaction (summation of Eqs. 1 and 2) can subsequently be expressed by

$$Li_xC_6 + S \rightarrow Li_{x-y}C_6 + yLiR + gas. \qquad [3]$$

As a result of this reaction sequence the graphite electrode is losing lithium under storage conditions and is, consequently, self-discharged.

Model development

Tunneling current

The above model is based on the assumption that the capacity loss is completely determined by the SEI formation on the negative electrode and that electron tunneling is rate-determining in the degradation process. The SEI formation rate can then be described by the tunneling current. The electron supply to the inner and outer SEI interface can be split into two steps. The electrons first have to be transported through the bulk of the graphite electrode to the electrode surface (28), followed by the tunneling process through the inner SEI layer.

Electron transport from the bulk to the electrode surface can be described by

$$dN = \frac{(6+x)N_A\rho_{C_6}}{4M_{C_6}}\upsilon_e A dt, \qquad [4]$$

where dN denotes the number of electron tunneling attempts during time dt [s], x is the normalized State-of-Charge ($0 < x \leq 1$), ρ_{C_6} the density of graphite [g·mol^{-1}], υ_e the velocity of the electrons moving in the bulk of graphite [m·s^{-1}], A the surface area of graphite available for electron tunneling [m^2], M_{C_6} the molar mass of graphite [g·mol^{-1}] and N_A is Avogadro's number [mol^{-1}]. 6 in the numerator of Eq. 4 corresponds to the number of free electrons per C_6 entity and 4 in the denominator comes from the assumption that the velocity vector of electrons within the graphene layers can take one of four orthogonal directions with equal probabilities (1/4).

A simple rectangular energy barrier model is used in the present model to describe the electron tunneling process across the inner SEI layer. The tunneling probability (P) can then be written as (28)

$$P = P_0 \exp\left(-\frac{2l^{in}\sqrt{2m\Delta E}}{\hbar}\right), \qquad [5]$$

where $\Delta E = U - E_f(x)$, U is the energy level related to vacuum, $E_f(x)$ is the Fermi level of the graphite electrode, the probability constant (P_0) is taken unity for simplicity, m the mass of electron and $\hbar$ is the reduced Planck constant. The tunneling current is the product of the tunneling probability and the electron density at the graphite surface. Combining Eqs. 4 and 5 the tunneling current I_t can be expressed as a function of State-of-Charge (x), according to

$$I_t = P\frac{dN}{dt}e = \frac{(6+x)F\rho_{C_6}}{4M_{C_6}}\upsilon_e A\ P_0 \exp\left(-\frac{2l^{in}\sqrt{2m\Delta E}}{\hbar}\right). \quad [6]$$

SEI formation during storage

In the case of storage, the capacity loss in the present model is completely determined by electron tunneling. It is assumed that the SoC is known ($x(t) = x$) and that the electron tunneling barrier is constant ($\Delta E(t) = \Delta E$). The SEI formation rate can then be expressed by

$$\frac{dQ_{SEI}^{st}(t)}{dt} = \frac{(6+x)F\rho_{C_6}A^{eq}}{4M_{C_6}}\upsilon_e P_0 \exp\left(-\frac{2\left(l_0^{in} + \frac{\delta Q_{SEI}^{st}(t)M_{Li}}{A^{eq}\rho^{in}w_{Li}^{in}F}\right)\sqrt{2m\Delta E}}{\hbar}\right), \quad [7]$$

where $Q_{SEI}^{st}(t)$ is the amount of Li captured in both SEI layers (summation of the inner and outer SEI) from time $t = 0$ up to storage time t [s], superscript st denotes storage, l_0^{in} [m] corresponds to the thickness of initial inner SEI layer formed on the graphite surface after activation, ρ^{in} [g·m^{-3}] is the gravimetric density of inner SEI layer, w_{Li}^{in} the weight percentage of Li in the inner SEI layer, M_{Li} [g· mol^{-1}] the molar mass of Li, F the Faraday constant and δ is the ratio between capacity of inner layer and total SEI layers. The ordinary differential equation given by Eq. 7 is simple and can be solved by a standard integration scheme, *e.g.* Euler.

Experimental

Pristine prismatic commercial 50 Ah batteries were used in the experiments. The chemical composition of the cathode and anode is $LiFePO_4$ and graphite (AG56-1), respectively. The electrochemical performance of the batteries was tested using automated cycling equipment (Maccor). All cells were activated for 4 cycles with a constant (dis)charge current of 5 A (0.1 C-rate). Subsequently, the batteries were fully charged and discharged under CCCV regimes in order to determine the maximum initial storage capacity $Q_{\max}^{ch}$ and $Q_{\max}^{d}$. The cut-off conditions were 3.65 V until the charging current reached 0.1 A $(1/500C)$, which is denoted as deep-charging, and 1.6 V until 0.1 A $(1/500C)$ for deep-discharging.

The batteries were charged to $Q_{ch}^{1} = 0.3\ Q_{\max}^{ch}$, $Q_{ch}^{1} = 0.7\ Q_{\max}^{ch}$ and $Q_{ch}^{1} = Q_{\max}^{ch}$ (the superscript refers to the first cycle after activation), and subsequently stored for 20 days. The batteries were deep-discharged after every 20 days and the corresponding deep-discharge capacities were noted as Q_{d}^{i} where i denotes the storage step. Thereafter the batteries were charged to the previously determined capacity ($Q_{ch}^{i+1} = Q_{d}^{i}$) after fully discharging in order to make sure all cells continue the previous storage experiment. All batteries were cycled and stored under temperature-controlled conditions (25°C).

Results and Discussion

The proposed model is validated by experiments. The Ordinary Least Squares method was used to estimate the unknown parameters. Both the experimentally observed capacity degradation data and the simulated results are showed in Fig. 2. The simulation results (solid lines) simulate the experimental data, stored at 30% SoC (red dots), 70% SoC (blue dots) and 100% SoC (magenta dots), very well. After storage at 30% SoC for 3000 hours the capacity decreased 0.935 Ah, approximately 2% of the initial value, while storage at 70% and 100% induced a two times higher degradation with losses of 1.844 Ah and 1.841 Ah, respectively. Under the present storage conditions it can be assumed that volume changes of the electrodes are considered negligible. Under these conditions the inner SEI layer will tightly cover the graphite surface and electrons can tunnel through this fixed layer continuously. As a result both the inner and outer SEI layer will continue to grow slowly. The capacity loss $Q_{SEI}(x,t)$ only depend on x and total storage time t.

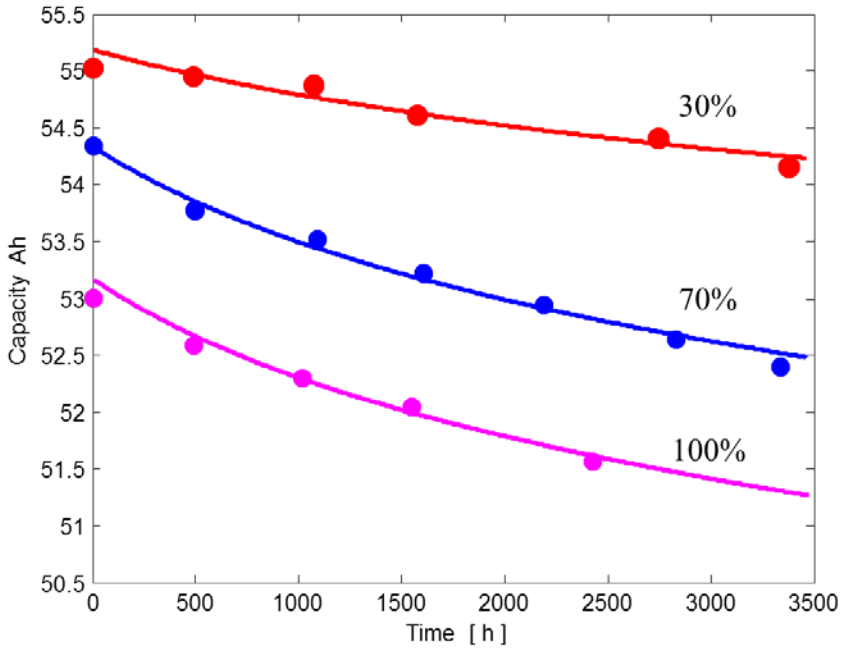

Fig. 2. Measured (symbols) and simulated (lines) capacity as a function of storage time.

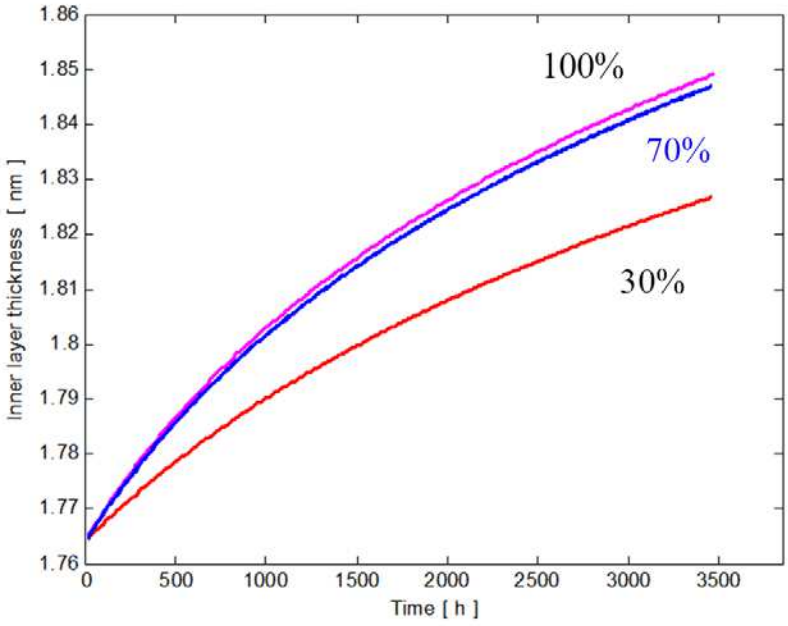

Fig. 3. Inner SEI layer growth under various storage conditions.

Fig. 3 shows the growth of the inner layer thickness upon storage. The main components of the inner SEI layer were attributed to inorganic Li salts (2). The thickness of the inner SEI layer has been analyzed by Edström *et al.* (14), using X-ray photoelectron spectroscopy (XPS). According to their study, the inner layer thickness is in a range of 15-20Å. The average thickness of the calculated inner SEI layer (see Fig. 3) is in good agreement with these experimental results. Though the factors affecting the inner SEI layer formation are still subject of debate, the electrode potential has a significant influence on the products of the SEI formation (18). When the cells were stored at 70% and 100% SoC, the electrode potential of the graphite electrode are very similar, resulting in a similar growth rate of the inner SEI layer. In the case of lower SoC storage (30%), *i.e.* when the graphite electrode voltages are more positive, the inner layer growth is obviously slower than at higher SoC.

Conclusions

In this work we developed an electron tunneling-based SEI formation model, which describes the experimentally observed capacity losses upon storage very well. The SEI layer consists of compact inner SEI layer and highly porous outer SEI layer. It is proposed that the SEI layers are grown at the interface of the inner and outer SEI layer at substantially different rates and that the overall rate is determined by the tunneling probability. The inner SEI layer plays a crucial role in protecting the electrode from exfoliation. The capacity losses are found to be largely dependent on the SoC and hence the electrode potential.

Acknowledgements

The China Scholarship Committee (CSC) is acknowledged for funding the first author to perform his study at the Department of Chemical Engineering and Chemistry of the Eindhoven University of Technology. The second and the last co-authors appreciate support from Eniac BATTMAN project.

References

1. D. Aurbach, B. Markovsky, I. Weissman, E. Levi and Y. Ein-Eli, *Electrochimica Acta*, **45**, 67 (1999).
2. D. Aurbach, *Journal of Power Sources*, **89**, 206 (2000).
3. D. Aurbach, E. Zinigrad, Y. Cohen and H. Teller, *Solid State Ionics*, **148**, 405 (2002).
4. P. Arora, R. E. White and M. Doyle, *Journal of the Electrochemical Society*, **145**, 3647 (1998).
5. S. Leroy, H. Martinez, R. Dedryvere, D. Lemordant and D. Gonbeau, *Applied Surface Science*, **253**, 4895 (2007).
6. M. Lu, H. Cheng and Y. Yang, *Electrochimica Acta*, **53**, 3539 (2008).
7. K. Xu and A. von Cresce, *Journal of Materials Chemistry*, **21**, 9849 (2011).
8. J. T. Lee, N. Nitta, J. Benson, A. Magasinski, T. F. Fuller and G. Yushin, *Carbon*, **52**, 388 (2013).
9. E. Peled, D. Golodnitsky, A. Ulus and V. Yufit, *Electrochimica Acta*, **50**, 391 (2004).
10. P. Verma, P. Maire and P. Novak, *Electrochimica Acta*, **55**, 6332 (2010).
11. S. Yamaguchi, H. Asahina, K. A. Hirasawa, T. Sato and S. Mori, *Molecular Crystals and Liquid Crystals Science and Technology Section a-Molecular Crystals and Liquid Crystals*, **322**, 239 (1998).
12. A. M. Andersson and K. Edstrom, *Journal of the Electrochemical Society*, **148**, A1100 (2001).
13. A. M. Andersson, M. Herstedt, A. G. Bishop and K. Edstrom, *Electrochimica Acta*, **47**, 1885 (2002).
14. A. M. Andersson, A. Henningson, H. Siegbahn, U. Jansson and K. Edstrom, *Journal of Power Sources*, **119**, 522 (2003).
15. K. Edstrom, M. Herstedt and D. P. Abraham, *Journal of Power Sources*, **153**, 380 (2006).
16. A. J. Smith, J. C. Burns, X. Zhao, D. Xiong and J. R. Dahn, *Journal of the Electrochemical Society*, **158**, S23 (2011).
17. F. M. Wang, M. H. Yu, Y. J. Hsiao, Y. Tsai, B. J. Hwang, Y. Y. Wang and C. C. Wan, *Int J Electrochem Sc*, **6**, 1014 (2011).
18. S. Leroy, F. Blanchard, R. Dedryvere, H. Martinez, B. Carre, D. Lemordant and D. Gonbeau, *Surface and Interface Analysis*, **37**, 773 (2005).
19. H. Bryngelsson, M. Stjerndahl, T. Gustafsson and K. Edstrom, *Journal of Power Sources*, **174**, 970 (2007).
20. J. Christensen and J. Newman, *Journal of the Electrochemical Society*, **151**, A1977 (2004).
21. E. Peled, *Journal of the Electrochemical Society*, **126**, 2047 (1979).
22. E. Peled, D. Golodnitsky and G. Ardel, *Journal of the Electrochemical Society*, **144**, L208 (1997).

23. J. Christensen and J. Newman, *Journal of the Electrochemical Society*, **152**, A818 (2005).
24. A. Awarke, S. Pischinger and J. Ogrzewalla, *Journal of the Electrochemical Society*, **160**, A172 (2013).
25. M. B. Pinson and M. Z. Bazant, *Journal of the Electrochemical Society*, **160**, A243 (2013).
26. Y. Xie, J. Li and C. Yuan, *Journal of Power Sources*, **248**, 172 (2014).
27. H. J. Ploehn, P. Ramadass and R. E. White, *Journal of the Electrochemical Society*, **151**, A456 (2004).
28. K. E. Heusler and K. S. Yun, *Electrochimica Acta*, **22**, 977 (1977).